Simultaneous Aromatic–Beryllium Bonds and Aromatic–Anion Interactions: Naphthalene and Pyrene as Models of Fullerenes, Carbon Single-Walled Nanotubes, and Graphene

ARTICLE *in* CHEMPHYSCHEM · JUNE 2015

Impact Factor: 3.42 · DOI: 10.1002/cphc.201500273 · Source: PubMed

ChemPubSoc Europe
DOI: 10.1002/cphc.201500273
CHEMPHYSCHEM Articles

Simultaneous Aromatic–Beryllium Bonds and Aromatic–Anion Interactions: Naphthalene and Pyrene as Models of Fullerenes, Carbon Single-Walled Nanotubes, and Graphene

Marta Marín-Luna,[a] Ibon Alkorta,*[a] José Elguero,[a] Otilia Mó,[b] and Manuel Yáñez*[b]

The possibility of forming stable BeR_2:ArH:Y^- (R = H, F, Cl; ArH = naphthalene, pyrene; Y = Cl, Br) ternary complexes in which the beryllium compounds and anions are located on the opposite sides of an extended aromatic system is explored by means of MP2/aug-cc-pVDZ ab initio calculations. Comparison of the electron-density distribution of these ternary complexes with the corresponding BeR_2:ArH and ArH:Y^- binary complexes reveals the existence of significant cooperativity between the two noncovalent interactions in the triads. The energetic effects of this cooperativity are quantified by evaluation of the three-body interaction energy Δ^3E in the framework of the many-body interaction-energy (MBIE) approach. Although an essential component of the interaction energies is electrostatic and is well reflected in the changes in the molecular electrostatic potential of the aromatic system on complexation, strong polarization effects, in particular for the BeR_2:ArH interactions, also play a significant role. The charge transfers associated with these polarization effects are responsible for significant distortion of both the BeR_2 and the aromatic moieties. The former are systematically bent in all the complexes, and the latter are curved to a degree that depends on the nature of the R substituents of the BeR_2 subunit.

1. Introduction

On the 150th anniversary of the Kekulé benzene structure,[1] it is worth remembering the three most important benzene derivatives of the 21st century: fullerenes, carbon nanotubes, and graphene. All of them can exist as insulators[2] by separating species of different charges (neutral, anionic, and cationic). However, due to their different geometries, the charged entities can adopt different arrangements (Figure 1).

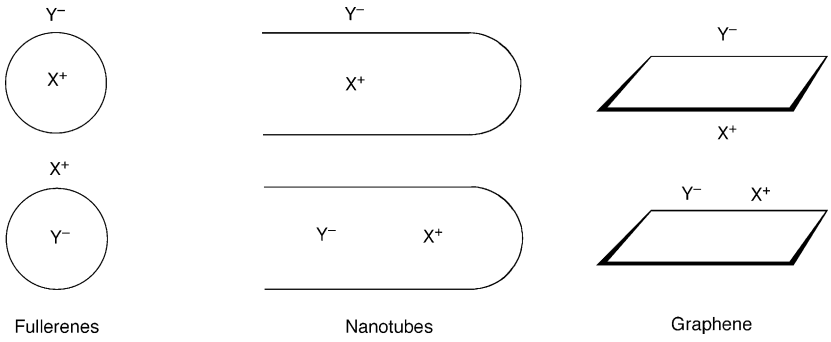

Figure 1. Ionic salts in endohedral fullerenes, nanotubes (only one possibility shown), and graphene.

Endohedral fullerenes such as $[Li@C_{60}]^+PF_6^-$ (also with other anions) are well known,[3] and the interaction of anions and cations through the fullerene wall has been explored theoretically.[4] In nanotubes, frequently the ions move inside the cavity to form salt crystallites,[5] whereas in graphene both ions remain on the same side.[6] Furthermore, the barrier for the permeation of BeH_2 through the central hexagon of coronene, as a model for extended graphene, has been calculated.[7]

Several authors have studied theoretically the possibility that aromatic and other π-system molecules could act as insulators between anions and cations: C_6H_6 and C_6F_6 between alkali metal cations and halide anions,[8] the bis-arene chromium complex [Cr(η-C_6H_6)(η-C_6F_6)] between alkali metal cations and halide anions,[9] tetrafluoroethene with anions and hydrogen-bond donors,[10] interaction of positively and negatively charged aromatic hydrocarbons with benzene and triphenylene,[11] cooperative effects between cation–π, anion–π, and π–π interactions,[12] and interplay between cation–π, anion–π,

[a] Dr. M. Marín-Luna, Prof. I. Alkorta, Prof. J. Elguero
Instituto de Química Médica (CSIC)
Juan de la Cierva, 3, 28006 Madrid (Spain)
E-mail: ibon@iqm.csic.es
Homepage: http://are.iqm.csic.es

[b] Prof. O. Mó, Prof. M. Yáñez
Departamento de Química, Módulo 13
Universidad Autónoma de Madrid
Campus de Excelencia UAM-CSIC
Cantoblanco, 28049 Madrid (Spain)
E-mail: manuel.yanez@uam.es

Supporting Information for this article is available on the WWW under http://dx.doi.org/10.1002/cphc.201500273.

and π–π interactions.[13] Cation–π and anion–π interactions have been reviewed,[14] and interactions with anions and cations have been extended to saturated rings (cyclohexane and adamantane).[15]

The possibility that beryllium compounds can interact with π systems has been explored recently by some of us: complexes between BeR_2 and ethylene and acetylene were considered.[16] Herein, the complexes with larger π systems such as naphthalene and pyrene are examined. In addition, the possibility of forming stable triads in which the beryllium compounds are located above one face of the π system and an anion is on the opposite face is explored.

Computational Methods

An initial exploration of the most suitable method to evaluate the aromatic systems treated in this article was carried out. The geometries of naphthalene and pyrene with D_{2h} symmetry were optimized at the MP2 level of theory[17–20] with different basis sets, and frequency calculations at the same level were performed to verify that the computational method considered does not predict imaginary frequencies.[21] The aug′-cc-pVDZ basis set, which corresponds to the aug-cc-pVDZ basis set for the heavy atoms and the cc-pVDZ basis set for the hydrogen atoms, was chosen.

The geometries of the complexes were optimized at the MP2/aug′-cc-pVDZ level of theory, and frequencies were obtained at the same level of theory to verify that the structures obtained correspond to energetic minima. Optimization and frequency calculations were performed with the Gaussian 09 program package.[22]

The many-body interaction-energy (MBIE) formalism[23,24] was applied to obtain the one-, two-, and three-body contributions to the binding energy (BE). For a ternary complex, ΔE can be decomposed into one-, two-, and three-body interactions [Eqs. (1)–(4)]:

$$\Delta E = E(\mathrm{ABC}) - \sum_{i=\mathrm{A}}^{\mathrm{C}} E_{\mathrm{m}}(i) = \sum_{i=\mathrm{A}}^{\mathrm{C}} [E(i) - E_{\mathrm{m}}(i)] + \sum_{i=\mathrm{A}}^{\mathrm{B}} \sum_{j>i}^{\mathrm{C}} \Delta^2 E(ij) + \Delta^3 E(\mathrm{ABC}) \quad (1)$$

$$E_{\mathrm{R}}(i) = E(i) - E_{\mathrm{m}}(i) \quad (2)$$

$$\Delta^2 E(ij) = E(ij) - [E(i) - E(j)] \quad (3)$$

$$\Delta^3 E(\mathrm{ABC}) = E(\mathrm{ABC}) - [E(\mathrm{A}) + E(\mathrm{B}) + E(\mathrm{C})] - [\Delta^2 E(\mathrm{AB}) + \Delta^2 E(\mathrm{AC}) + \Delta^2 E(\mathrm{BC})] \quad (4)$$

where $E_m(i)$ is the energy of an isolated, optimized monomer, $E(i)$ the energy of the monomer at its geometry in the complex, $E_R(i)$ the distortion energy of the monomer, and $\Delta^2E(ij)$ and $\Delta^3E(\mathrm{ABC})$ are the two- and three-body interaction energies calculated at the corresponding geometries in the complex.

Molecular electrostatic potentials (MEPs) were calculated by using Gaussian 09 and an in-house program to evaluate this parameter on the 0.001 a.u. electron-density isosurface.

The electron densities of complexes were analyzed by using the Atoms in Molecules (AIM) methodology[25–28] as implemented in the AIMAll[29] program. The atomic charges were calculated by numerical integration in the atomic basins. The quality of the charges was assessed in terms of the value of the integrated Laplacian, which should ideally be zero in the atomic basins.[30] A complementary view of the bonding was obtained through use of the Natural Bond Orbital (NBO) approach. In this method the bonding of a molecular system is described in terms of localized hybrids, so that a second-order perturbation treatment permits the interaction energies between occupied and empty orbitals to easily be obtained. When these orbitals belong to different subunits of a molecular aggregate bound by noncovalent interactions, as in our case, the aforementioned interaction energies give a clear idea of charge donations and backdonations between the interacting moieties. These NBO calculations were carried out at the B3LYP/aug-cc-pVDZ level of theory.

2. Results and Discussion

2.1. Binary Complexes

This section focuses on the complexes between the aromatic systems and beryllium compounds or anions located above the aromatic ring. All these complexes show C_{2v} symmetry. All the structures are minima, except for the naphthalene:anion complexes, which have one imaginary frequency. The latter complexes show a minimum-energy configuration in which the anions lie in the molecular plane, where they interact simultaneously with two CH groups. Here, we discuss the structure of the naphthalene:anion complexes with one imaginary frequency, since they are similar to the corresponding ternary complexes analyzed below.

The BEs of the binary complexes are listed in Table 1. The energies of the $ArH:Y^-$ complexes range between −7 and −22 kJ mol^{-1}. The BE increases with increasing size of the aromatic ring and increasing size of the anion. Thus, the stabilization is greater for the pyrene complexes than for the corresponding naphthalene complexes, and the bromide complexes have more negative BEs than the chloride complexes. The intermolecular distances parallel the energetic results by being shorter for pyrene complexes than for the naphthalene ana-

Table 1. BEs [kJ mol^{-1}], distances [Å] from Be/Y^- to the center of the interacting C–C bond (Z), and R–Be–R angles [°].

	BE		$Be/Y^-\cdots Z$ distance		R–Be–R angle	
	ArH = naphthalene	ArH = pyrene	ArH = naphthalene	ArH = pyrene	ArH = naphthalene	ArH = pyrene
$ArH:Cl^-$	−6.7[a]	−17.5	3.284	3.115		
$ArH:Br^-$	−10.1[a]	−21.6	3.445	3.272		
$ArH:BeH_2$	−24.9	−30.8	2.608	2.539	164.3	163.6
$ArH:BeF_2$	−31.7	−40.4	2.429	2.363	149.9	149.1
$ArH:BeCl_2$	−36.0	−49.5	2.607	2.410	148.1	141.5

[a] These complexes have one imaginary frequency.

logues and for bromide complexes compared to chloride complexes.

The BeR_2:ArH complexes show BEs between −25 and −50 kJ mol^{-1}. As in the case of the anions, the stabilization of the complex increases with increasing size of the aromatic ring or beryllium compound. However, in this case, the intermolecular distances are shorter for the BeF_2 complexes than for the $BeCl_2$ complexes, even though the BE is smaller in absolute value in the latter complexes. The longest distances are found for the BeH_2 complexes of both naphthalene and pyrene.

Complex formation results in geometrical changes in the beryllium compounds, with elongation of the Be–R bond by 0.03 Å in the pyrene:$BeCl_2$ complex, and the R–Be–R arrangement is no longer linear, with a bond angle of 141° in the same complex. In the same way, the aromatic derivatives tend to bend, whereby the outer atoms move away from the beryllium substituents (Scheme 1) with values of α up to 174°. In the complexes with the anions, the observed curvature of the aromatic systems is very small, less than 1°, and in the opposite direction to that observed in the binary BeR_2 complexes.

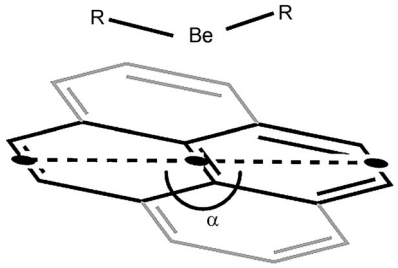

Scheme 1. Definition of α.

To analyze the effect of the distortion and the interaction energy, the MBIE partition was considered for the binary complexes (Table 2). The distortion energies of the monomers in the complexes are small for the aromatic systems (between 0.7 and 3.7 kJ mol^{-1}), whereas those for the beryllium compounds depend on the substituents and range between 5 and 34 kJ mol^{-1}. The largest distortions are obtained for the $BeCl_2$ complexes, and the smallest for the BeH_2 complexes. Consequently, the interaction energies Δ^2E in the $BeCl_2$ complexes are more than twice those of the analogous complexes with BeH_2. The BeF_2 complexes show intermediate distortions and interaction energies to those of BeH_2 and $BeCl_2$.

Table 2. MBIE partition terms [kJ mol^{-1}].[a]

	E_R(ArH)	E_R(BeR_2/Y^-)	Δ^2E(AB)
naphthalene:Cl^-	0.7	0.0	−7.4
naphthalene:Br^-	0.7	0.0	−10.8
pyrene:Cl^-	1.9	0.0	−19.3
pyrene:Br^-	1.9	0.0	−23.5
naphthalene:BeH_2	0.3	5.1	−30.4
naphthalene:BeF_2	0.9	20.2	−52.8
naphthalene:$BeCl_2$	2.1	22.9	−61.0
pyrene:BeH_2	0.6	5.6	−37.1
pyrene:BeF_2	1.3	21.3	−63.1
pyrene:$BeCl_2$	3.7	33.9	−87.2

[a] The sum of these terms is equal to the BE.

The topological analysis of the electron density of the binary complexes shows a single intermolecular bond path between the anions and the aromatic systems, whereas in the case of the beryllium compounds, all of the atoms of these molecules interact with the aromatic system, as shown in Figure 2, with the exception of the BeH_2, for which no bond path is found between the beryllium atom and the π system. The molecular graphs of all complexes are shown in Figure S1 of the Supporting Information.

The association of halide anions or BeR_2 with the aromatics leads to electron-density redistributions triggered by the polarization of the electron clouds of both interacting subunits. These polarization effects can be detected by looking at the charge transfer between the two moieties. This charge transfer was quantified by using the natural charges obtained with the NBO approach. The values obtained (see Table 3) show that for all the BeR_2 binary complexes the aromatic moiety has a net positive charge, whereas for complexes with halide anions the net charge is negative, and it is more negative in the pyrene complexes than in the naphthalene complexes. These values indicate that in complexes with BeR_2 the aromatic moiety behaves as a Lewis base, whereas it behaves as a Lewis acid on interacting with halide anions. Indeed, the NBO second-order orbital interaction energies show that in complexes with BeR_2 the interactions involve occupied π_{CC} bonding orbitals of the aromatic moiety and the empty orbitals of the BeR_2 subunit, predominantly the empty 2p orbital of Be (interaction energy: 40 kJ mol^{-1} for naphthalene:BeH_2) and secondarily with the σ^*_{BeR} antibonding orbital (interaction energy: 4 kJ mol^{-1} for naphthalene:BeH_2). The former interactions are responsible for the bending of the BeR_2 moiety, because of the hybridization change associated with population of the 2p orbital, and for slight lengthening of the Be–R bonds. For complexes with halide anions, the main orbital interaction involves the lone pairs of the halogen atom and the π^*_{CC} antibonding orbitals of the aromatic (interaction energy: 3 kJ mol^{-1} for naphthalene:Cl^-)

Table 3. Natural charges [e] of the aromatic systems in the binary complexes.

System	ArH = naphthalene	ArH = pyrene
ArH:BeH_2	0.041	0.038
ArH:BeF_2	0.036	0.034
ArH:$BeCl_2$	0.061	0.071
ArH:Cl^-	−0.015	−0.029
ArH:Br^-	−0.012	−0.024

These electron-density redistributions necessarily affect the electrostatic potential of the aromatic system on the face opposite that at which the interaction takes place, and therefore the stability of ternary complexes in which the aromatic system interacts simultaneously with beryllium compounds

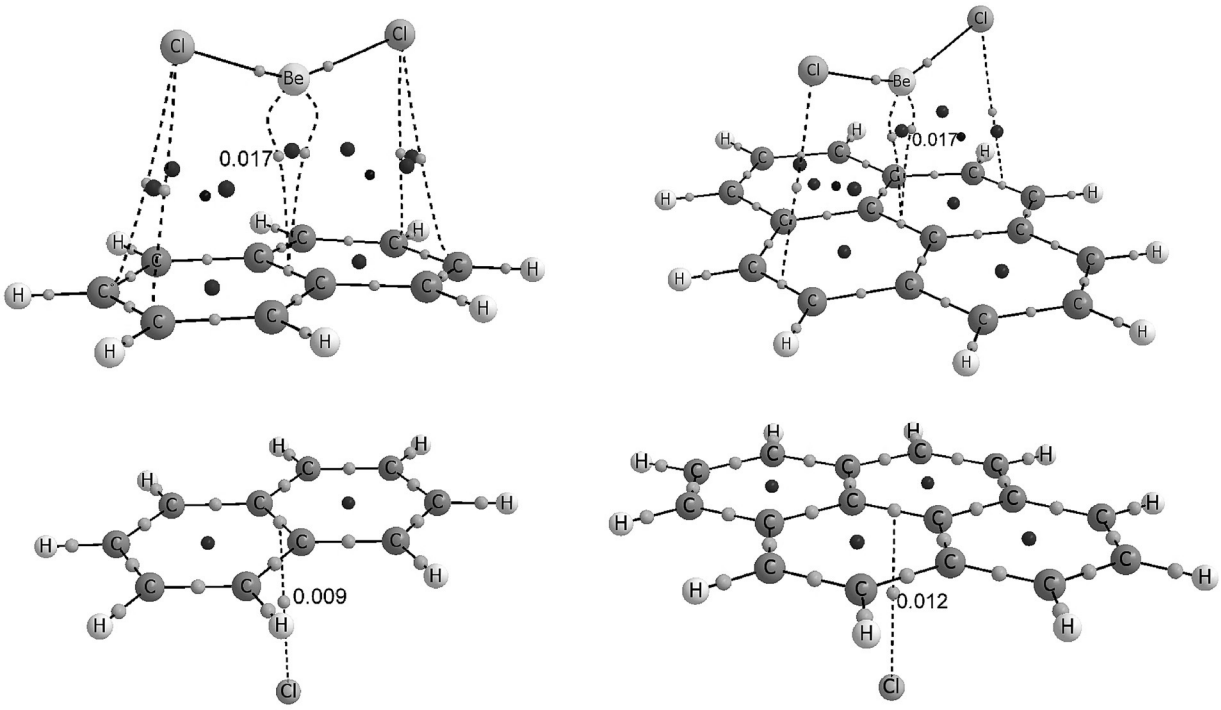

Figure 2. Molecular graph of some representative binary complexes between the π systems (naphthalene and pyrene) and the beryllium compounds or anions (chloride and bromide). Gray, large black, and small black circles denote bond critical points (BCPs), ring critical points (RCPs), and cage critical points (CCPs), respectively.

and halide anions. To quantify this effect, we evaluated the electrostatic potential along the symmetry axis perpendicular to the aromatic systems at an electron density of 0.001 a.u. at the face opposite to the interacting molecule. The values obtained (Table 4) show that complexation of the aromatic molecules with anions makes the electrostatic potential on the other face much more negative (see Table 4). In contrast, the opposite effect is observed for complexation with BeR_2 and leads to electrostatic potentials that are significantly less negative than for the isolated aromatic (see Table 4). These results indicate that the ArH:Y^- binary complexes should form stronger complexes with beryllium complexes than the isolated aromatic systems. Similarly, the BeR_2:ArH binary complexes should also yield stronger associations with the anions than the isolated ones.

Table 4. Electrostatic potential [kJ mol^{-1}] along the symmetry axis perpendicular to the aromatic ring opposite to the interacting molecule on the 0.001 a.u. electron-density isosurface.

	ArH = naphthalene	ArH = pyrene
ArH	−55	−52
ArH:Cl^-	−341	−331
ArH:Br^-	−333	−323
ArH:BeH_2	−29	−26
ArH:BeF_2	−10	−11
ArH:$BeCl_2$	−10	−3

2.2. Ternary Complexes

The optimized structures of all ternary complexes BeR_2:ArH:Y^- (R = H, F, Cl; ArH = naphthalene, pyrene; Y = Cl, Br) show C_{2v} symmetry and are minima on the potential-energy surface (Figure 3). The BEs and intermolecular distances of these complexes are listed in Table 5. The BEs range between −57 and −118 kJ mol^{-1}. As in the case of the binary complexes, the larger the size of each of the components (aromatic system, anion, or beryllium compound), the higher the BE. Thus, the weakest complex is Cl^-:naphthalene:BeH_2, and the strongest is Br^-:pyrene:$BeCl_2$. This seems to indicate that dispersion is a non-negligible contributor to the BE for the anions, whereby the Br^- BEs are slightly larger than the Cl^- ones. Although for BeR_2 the differences in the BEs as a function of R are essentially due to the increase in the electron-acceptor capacity of the system when H is replaced by F or Cl, the greater dispersion expected for the latter also contributes to these differences.

In what follows, the distances between BeR_2 or Y^- and the aromatic system is measured as the distance between the Be or the Y atom and a dummy atom Z located at the midpoint of the central C–C bond of the aromatic.

The Ar···Be distances in the ternary complexes are very similar for a given BeR_2 molecule. With the sole exception of the $BeCl_2$:pyrene:Y^- complex, this distance is slightly longer for the complexes with Y = Br than for Y = Cl, which is in agreement with the electrostatic potentials listed in Table 3, which show that for the binary complexes this potential is slightly less negative for Br^- than for Cl^-. For a given halide anion, the Ar···Be distance decreases, by up to 0.12 Å, as a function of the sub-

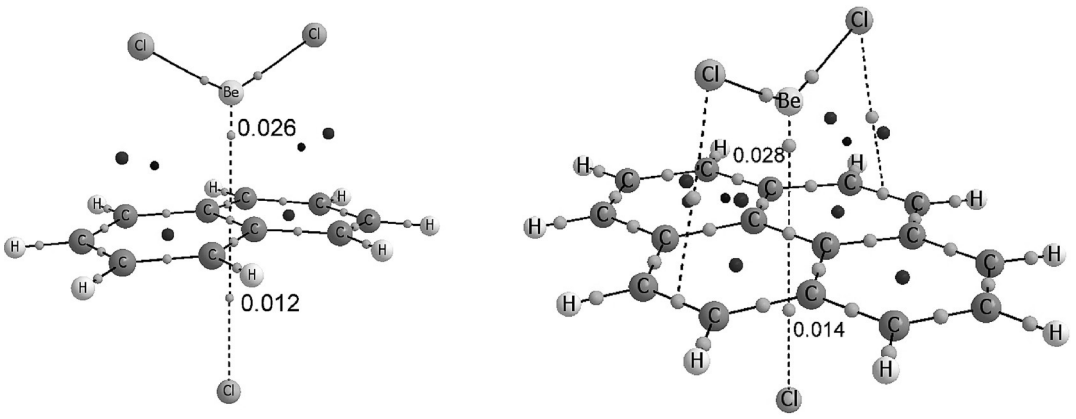

Figure 3. Molecular graph of two representative ternary complexes optimized at the MP2/aug′-cc-pVDZ level of theory. Gray, large black, and small black circles denote BCPs, RCPs, and CCPs, respectively.

Table 5. Binding energies (BE) [kJ mol^{-1}], intermolecular distances in the ternary complexes [Å], and R–Be–R angles [°].

	ArH = Naphthalene				ArH = Pyrene			
	BE	Be···Z[a]	Y$^-$···Z	R–Be–R	BE	Be···Z	Y$^-$···Z	R–Be–R
Cl$^-$:ArH:BeH$_2$	−57.2	2.286	3.173	146.0	−73.9	2.275	3.053	147.2
Br$^-$:ArH:BeH$_2$	−60.2	2.291	3.338	146.5	−78.1	2.276	3.211	147.5
Cl$^-$:ArH:BeF$_2$	−76.6	2.205	3.139	135.0	−94.4	2.183	3.026	135.9
Br$^-$:ArH:BeF$_2$	−79.3	2.207	3.300	135.4	−98.6	2.186	3.192	136.3
Cl$^-$:ArH:BeCl$_2$	−91.3	2.164	3.115	126.2	−114.1	2.148	3.022	126.9
Br$^-$:ArH:BeCl$_2$	−93.5	2.168	3.279	126.6	−118.0	2.146	3.121	127.2

[a] Z represents a dummy atom in the middle of the C–C bond involved in the interaction

stituent attached to Be: H > F > Cl. The intermolecular distance between the anions and the aromatic rings decreases slightly with increasing size of the substituents attached to Be and is always shorter in the pyrene complexes than in the naphthalene analogues. However, the most significant structural feature is the drastic shortening of these distances on going from the binary to the ternary complexes. The distance between the beryllium compound and the aromatic ring decreases by 0.18 to 0.44 Å, and the distance between the halide anion and the aromatic ring by 0.06 to and 0.17 Å. This shortening effect is slightly more pronounced in the naphthalene complexes than in the pyrene complexes.

The aforementioned structural changes are a direct consequence of the cooperative effect of the two noncovalent interactions on the electron-density distribution of the triad. Indeed, an NBO analysis showed that donation from the π_{CC} occupied bonding orbitals of the aromatic to the empty 2p orbital of Be and the σ^*_{BeR} antibonding orbital of the BeR_2 subunit significantly increase on going from binary to ternary complexes. Let us take the BeH_2:naphthalene:Cl$^-$ complex as an example, for the sake of direct comparison with the values reported above for the BeH_2:naphthalene and naphthalene:Cl$^-$ binary complexes. In the ternary complex the second-order orbital interaction energy between the π_{CC} occupied bonding orbitals of the aromatic and the empty 2p orbital of Be is 149 kJ mol^{-1}, which is more than 100 kJ mol^{-1} larger than in the BeH_2:naphthalene binary complex. Similarly the interaction energy involving the σ^*_{BeX} antibonding orbital is 8 kJ mol^{-1}, that is, twice the value in the binary complex. Consistently, the electron density at the Be···Z BCP also increases, from 0.012 a.u. in the binary complex (see Figure S1) to 0.018 a.u. in the triad, and this leads to the observed shortening of the corresponding internuclear distances, in agreement with the correlations between electron density and interatomic distances already reported in the literature.[31–39]

The changes observed for the interaction between the aromatic and the halide anion are much smaller, which seems to be consistent with a predominance of electrostatic and dispersion terms. Nevertheless, the interaction energy between the lone pairs of Cl$^-$ and the π^*_{CC} antibonding orbitals of naphthalene still increases by 1 kJ mol^{-1} on going from the binary to the ternary complex. Also in this case a clear increase of the electron density at the Z···Cl$^-$ BCP on going from the binary to the ternary complex is observed (0.009 a.u. versus 0.011 a.u.). Hence, the shortening of the Be···Z distance is significantly larger than that of the Z···Y$^-$ distance, which indicates a dominant contribution of the former to stabilization of the triads. Consistent with the dominant role of the BeR_2:ArH interactions with respect to the ArH:Y$^-$ interactions is the fact that the curvature of the aromatic rings, already observed in the binary complexes, is even more pronounced in the ternary ones. In the case of the $BeCl_2$:ArH:Br$^-$ complexes, the angle α (Scheme 1) is 171° for both aromatic systems. A similar trend is observed in the R–Be–R angles, which have values

close to 130° in the ternary complexes (127° in the $BeCl_2$:ArH:Br^- complexes).

Moreover, the calculated net charges of the aromatic systems in the ternary complexes (see Table 6) are consistent with the dominant role of the BeR_2:ArH interaction in the triads. Not only are all the values positive, but they are also always larger than in the binary analogues. When the global net charge is decomposed into the components originating from the BeR_2:ArH and ArH:Y^- interactions, both are larger, in absolute value, than in the corresponding binary complexes (compare the values in Table 6 with those in Table 3), but the increase is much larger in the former case (by about a factor of three) than in the latter (by about a factor of 1.5).

The different terms of the MBIE partition, summarized in Table 7, are consistent with the above-discussed electron-density viewpoint. The first interesting feature is that the distortion energies of the beryllium compounds in the triads are more than twice those found in the binary complexes. The two-body energies show the ranking $\Delta^2E(Ar{:}BeR_2) < \Delta^2E(BeR_2{:}Y^-) < \Delta^2E(Ar{:}Y^-)$, and the three-body terms are always negative, with values between −1 and −18 kJ mol^{-1}. Overall, the $\Delta^2E(Ar{:}BeR_2)$ term represents more than half of the sum of all the attractive terms (between 50 and 63%) and the $\Delta^2E(BeR_2{:}Y^-)$ term between 20 and 30% of the attractive term. The other two terms are much more variable, with contribution between 3 and 23% for the $\Delta^2E(Ar{:}Y^-)$ term and 1 and 13% for the Δ^3E term.

A comparison with the values obtained for the binary complexes indicates that for the ternary complexes the $\Delta^2E(Ar{:}BeR_2)$ term is 34–73% larger than the same term in the analogous binary complexes. In contrast, the $\Delta^2E(Ar{:}Y^-)$ terms in the ternary complexes are less negative (by up to 23% in the naphthalene complexes and 3% in the pyrene complexes).

3. Conclusions

We have shown that it is possible to form stable BeR_2:ArH:Y^- (R = H, F, Cl; ArH = naphthalene, pyrene; Y = Cl, Br) ternary complexes in which the beryllium compounds and anions are located on the opposite sides of extended aromatic systems. Indeed, the association of BeR_2 or Y^- with the aromatics leads to a change in the electrostatic potential created by the aromatic on its free side. The potential becomes more negative when the association involves Y^- and more positive when it involves BeR_2. Hence binary complexes BeR_2:ArH should associate more strongly with Y^- anions than the isolated aromatic system. Similarly, ArH:Y^- binary complexes should be attached more strongly to BeR_2 compounds than the isolated aromatic compound. Coherently, a comparison of the electron-density distribution of the BeR_2:ArH:Y^- ternary complexes with the corresponding BeR_2:ArH and ArH:Y^- binary complexes shows the existence of significant cooperativity between the two noncovalent interactions in the triads. The energetic effects of this cooperativity were quantified by evaluation of the three-body interaction energy Δ^3E by the MBIE approach. Although an essential component of the interaction energies is electrostatic, which is well reflected in the changes in the molecular electrostatic potential of the aromatic system on complexation, strong polarization effects, in particular for the BeR_2:ArH interactions, also play a significant role. The charge transfers associated with these polarization effects are responsible for significant distortion of both the BeR_2 and the aromatic moieties. The former are systematically bent in all of the complexes, and the latter are curved to a degree that depends on the nature of the R substituents of the BeR_2 subunit.

Table 6. Natural charges of the aromatic systems [e] in the ternary complexes. The two values in brackets correspond to the contributions associated with the BeR_2:ArH and ArH:Y^- interactions, respectively.

	ArH = naphthalene		ArH = pyrene	
	Y = Cl	Y = Br	Y = Cl	Y = Br
BeH_2:ArH:Y^-	0.091 [0.116, −0.025]	0.090 [0.112, −0.022]	0.064 [0.101, −0.037]	0.066 [0.099, −0.033]
BeF_2:ArH:Y^-	0.069 [0.095, −0.026]	0.069 [0.092, −0.023]	0.045[0.081,−0.036]	0.048 [0.078, −0.031]
$BeCl_2$:ArH:Y^-	0.139 [0.168, −0.029]	0.138 [0.164, −0.026]	0.108 [0.146, −0.038]	0.109 [0.143, −0.034]

Table 7. MBIE terms [kJ mol^{-1}] in the ternary complexes.

	E_R(ArH)	E_R(BeR_2)	Δ^2E(ArH:BeR_2)	Δ^2E[ArH:Y^-]	Δ^2E(BeR_2:Y^-)	Δ^3E
Cl^-:naphthalene:BeH_2	1.78	25.13	−45.52	−6.62	−21.06	−10.94
Br^-:naphthalene:BeH_2	1.88	24.32	−45.07	−10.24	−19.67	−11.37
Cl^-:naphthalene:BeF_2	2.31	49.48	−77.31	−6.15	−37.9	−7.06
Br^-:naphthalene:BeF_2	2.46	48.58	−76.79	−9.78	−35.76	−8.02
Cl^-:naphthalene:$BeCl_2$	5.34	72.61	−105.65	−5.63	−39.93	−17.99
Br^-:naphthalene:$BeCl_2$	5.56	71.3	−104.88	−9.5	−37.58	−18.37
Cl^-:pyrene:BeH_2	2.00	23.35	−52.07	−19.14	−21.89	−6.13
Br^-:pyrene:BeH_2	2.16	22.93	−51.82	−23.48	−20.63	−7.27
Cl^-:pyrene:BeF_2	2.64	47.25	−85.08	−18.79	−39.64	−0.81
Br^-:pyrene:BeF_2	2.85	46.35	−84.5	−23.28	−37.28	−2.71
Cl^-:pyrene:$BeCl_2$	5.60	70.21	−119.53	−18.88	−41.55	−9.97
Br^-:pyrene:$BeCl_2$	5.83	69.44	−119.01	−23.02	−39.54	−11.66

Acknowledgements

This work has been partially supported by the Ministerio de Economía y Competitividad (Projects No. CTQ2012-35513-C02 and CTQ2013-43698-P), the Project FOTOCARBON, Ref.: S2013/MIT-2841 of the Comunidad Autónoma de Madrid, and by the CMST COST Action CM1204. A generous allocation of computing time at the CTI (CSIC) and at the CCC of the UAM is also acknowledged.

Keywords: ab initio calculations · anions · beryllium · cooperative effects · noncovalent interactions

[1] A. J. Rocke, *Angew. Chem. Int. Ed.* **2015**, *54*, 46 – 50; *Angew. Chem.* **2015**, *127*, 46 – 51.
[2] J. B. Oostinga, H. B. Heersche, X. Liu, A. F. Morpurgo, L. M. K. Vandersypen, *Nat. Mater.* **2008**, *7*, 151 – 157.
[3] a) S. Aoyagi, E. Nishibori, H. Sawa, K. Sugimoto, M. Takata, Y. Miyata, R. Kitaura, H. Shinohara, H. Okada, T. Sakai, Y. Ono, K. Kawachi, K. Yokoo, S. Ono, K. Omote, Y. Kasama, S. Ishikawa, T. Komuro, H. Tobita, *Nat. Chem.* **2010**, *2*, 678 – 683; b) H. Ueno, K. Kokubo, E. Kwon, Y. Nakamura, N. Ikuma, T. Oshima, *Nanoscale* **2013**, *5*, 2317 – 2321; c) A. A. Popov, S. Yang, L. Dunsch, *Chem. Rev.* **2013**, *113*, 5989 – 6113; d) E. Kwon, K.-I. Komatsu, K. Kawachi, Y. Kasama, T. Endo, *Mol. Cryst. Liq. Cryst.* **2014**, *598*, 28 – 31.
[4] F. De Proft, C. VanAlsenoy, P. Geerlings, *J. Phys. Chem.* **1996**, *100*, 7440 – 7448.
[5] M. Wilson, *J. Chem. Phys.* **2002**, *116*, 3027 – 3041.
[6] A. S. Pensado, F. Malberg, M. F. Costa Gomes, A. A. H. Pádua, J. Fernández, B. Kirchner, *RSC Adv.* **2014**, *4*, 18017 – 18024.
[7] S. E. Huber, M. Probst, *Int. J. Mass Spectrom.* **2014**, *365 – 366*, 248 – 254.
[8] I. Alkorta, J. Elguero, *J. Phys. Chem. A* **2003**, *107*, 9428 – 9433.
[9] I. Alkorta, D. Quiñonero, C. Garau, A. Frontera, J. Elguero, P. M. Deyà, *J. Phys. Chem. A* **2007**, *111*, 3137 – 3142.
[10] I. Alkorta, F. Blanco, J. Elguero, C. Estarellas, A. Frontera, D. Quiñonero, P. M. Deyà, *J. Chem. Theory Comput.* **2009**, *5*, 1186 – 1194.
[11] D. Quiñonero, A. Frontera, P. M. Deyà, I. Alkorta, J. Elguero, *Chem. Phys. Lett.* **2008**, *460*, 406 – 410.
[12] A. Frontera, D. Quiñonero, A. Costa, P. Ballester, P. M. Deyà, *New J. Chem.* **2007**, *31*, 556 – 560.
[13] D. Quiñonero, A. Frontera, C. Garau, P. Ballester, A. Costa, P. M. Deyà, *ChemPhysChem* **2006**, *7*, 2487 – 2491.
[14] A. Frontera, D. Quiñonero, P. M. Deyà, *Wiley Interdiscip. Rev. Comput. Mol. Sci.* **2011**, *1*, 440 – 459.
[15] C. Trujillo, G. Sanchez-Sanz, I. Alkorta, J. Elguero, *J. Phys. Chem. A* **2011**, *115*, 13124 – 13132.
[16] E. Fernández Villanueva, O. Mó, M. Yáñez, *Phys. Chem. Chem. Phys.* **2014**, *16*, 17531 – 17536.
[17] J. A. Pople, J. S. Binkley, R. Seeger, *Int. J. Quantum Chem. Quantum Biol. Symp.* **1976**, *10*, 1 – 19.
[18] R. Krishnan, J. A. Pople, *Int. J. Quantum Chem.* **1978**, *14*, 91 – 100.
[19] R. J. Bartlett, D. M. Silver, *J. Chem. Phys.* **1975**, *62*, 3258 – 3268.
[20] R. J. Bartlett, G. D. Purvis, *Int. J. Quantum Chem.* **1978**, *14*, 561 – 581.
[21] D. Moran, A. C. Simmonett, F. E. Leach, W. D. Allen, P. v. R. Schleyer, H. F. Schaefer III, *J. Am. Chem. Soc.* **2006**, *128*, 9342 – 9343.
[22] Gaussian 09, Revision D.01, M. J. Frisch, G. W. Trucks, H. B. Schlegel, G. E. Scuseria, M. A. Robb, J. R. Cheeseman, G. Scalmani, V. Barone, B. Mennucci, G. A. Petersson, H. Nakatsuji, M. Caricato, X. Li, H. P. Hratchian, A. F. Izmaylov, J. Bloino, G. Zheng, J. L. Sonnenberg, M. Hada, M. Ehara, K. Toyota, R. Fukuda, J. Hasegawa, M. Ishida, T. Nakajima, Y. Honda, O. Kitao, H. Nakai, T. Vreven, J. Montgomery, J. A., J. E. Peralta, F. Ogliaro, M. Bearpark, J. J. Heyd, E. Brothers, K. N. Kudin, V. N. Staroverov, R. Kobayashi, J. Normand, K. Raghavachari, A. Rendell, J. C. Burant, S. S. Iyengar, J. Tomasi, M. Cossi, N. Rega, N. J. Millam, M. Klene, J. E. Knox, J. B. Cross, V. Bakken, C. Adamo, J. Jaramillo, R. Gomperts, R. E. Stratmann, O. Yazyev, A. J. Austin, R. Cammi, C. Pomelli, J. W. Ochterski, R. L. Martin, K. Morokuma, V. G. Zakrzewski, G. A. Voth, P. Salvador, J. J. Dannenberg, S. Dapprich, A. D. Daniels, Ö. Farkas, J. B. Foresman, J. V. Ortiz, J. Cioslowski and D. J. Fox, Gaussian, Inc., Wallingford CT, 2009.
[23] D. Hankins, J. W. Moskowitz, F. H. Stillinger, *J. Chem. Phys.* **1970**, *53*, 4544 – 4554.
[24] S. Xantheas, *J. Chem. Phys.* **1994**, *100*, 7523 – 7534.
[25] R. F. W. Bader, *Chem. Rev.* **1991**, *91*, 893 – 928.
[26] R. F. W. Bader, *Atoms in Molecules, A Quantum Theory*, Oxford University Press, Oxford, **1990**.
[27] P. L. A. Popelier, *Atoms In Molecules. An introduction*, Prentice Hall, Harlow, **2000**.
[28] C. F. Matta, R. J. Boyd, *The Quantum Theory of Atoms in Molecules: From Solid State to DNA and Drug Design*, Wiley-VCH, Weinham, **2007**.
[29] AIMAll (Version 11.08.23), T. A. Keith, TK Gristmill Software, Overland Park KS, USA, 2011 (http://aim.tkgristmill.com).
[30] I. Alkorta, O. Picazo, *ARKIVOC (Gainesville, FL, U.S.)* **2005**, *2005*, 305 – 320.
[31] O. Knop, R. J. Boyd, S. C. Choi, *J. Am. Chem. Soc.* **1988**, *110*, 7299 – 7301.
[32] G. V. Gibbs, F. C. Hill, M. B. Boisen, R. T. Downs, *Phys. Chem. Miner.* **1998**, *25*, 585 – 590.
[33] I. Alkorta, L. Barrios, I. Rozas, J. Elguero, *J. Mol. Struct. THEOCHEM* **2000**, *496*, 131 – 137.
[34] O. Knop, K. N. Rankin, R. J. Boyd, *J. Phys. Chem. A* **2001**, *105*, 6552 – 6566.
[35] O. Knop, K. N. Rankin, R. J. Boyd, *J. Phys. Chem. A* **2003**, *107*, 272 – 284.
[36] E. Espinosa, I. Alkorta, J. Elguero, E. Molins, *J. Chem. Phys.* **2002**, *117*, 5529 – 5542.
[37] I. Alkorta, J. Elguero, *Struct. Chem.* **2004**, *15*, 117 – 120.
[38] T. H. Tang, E. Deretey, S. J. K. Jensen, I. G. Csizmadia, *Eur. Phys. J. D* **2006**, *37*, 217 – 222.
[39] I. Mata, I. Alkorta, E. Molins, E. Espinosa, *Chem. Eur. J.* **2010**, *16*, 2442 – 2452.

Received: March 30, 2015
Published online on June 30, 2015